Sensing Performance of Different Codes for Phase-Coded FMCW Radars

Kumbul, Utku; Petrov, Nikita; Vaucher, Cicero S.; Yarovoy, Alexander

DOI
10.23919/EuRAD54643.2022.9924751

Publication date
2022

Document Version
Final published version

Published in
2022 19th European Radar Conference, EuRAD 2022

Sensing Performance of Different Codes for Phase-Coded FMCW Radars

Utku Kumbul[#1], Nikita Petrov[*#2], Cicero S. Vaucher[*#3], Alexander Yarovoy[#4]

[#] Department of Microelectronics, Delft University of Technology, Delft, The Netherlands

[*] NXP Semiconductors, Eindhoven, The Netherlands

{[1]u.kumbul, [2]n.petrov, [3]c.silveiravaucher, [4]a.yarovoy}@tudelft.nl

***Abstract* — The sensing properties of the binary phase codes are investigated with their application to phase-coded (linearly) frequency modulated continuous waveform (PC-FMCW). It is shown that the ambiguity function of FMCW signal modulated with a binary phase code corresponds to sheared ambiguity function of the code itself. The range profiles of PC-FMCW with different code families are analysed and compared in terms of integrated sidelobe level (ISL).**

***Keywords* — Phase modulation, Modulated chirps, Ambiguity function, Phase-coded FMCW.**

I. Introduction

Linear frequency modulated continuous waveforms (LFMCW) have been used in many radar applications as it provides high range resolution, low sidelobes, good Doppler tolerance and constant peak-to-average power ratio (PAPR) with a relatively low hardware complexity [1]. However, these benefits come with the price of having poor distinctness, which makes the LFM waveform weak against radar to radar interference [2]. In addition, the orthogonality between waveforms is crucial for the realization of multiple input multiple output (MIMO) systems, and creating mutual orthogonality between LFMCW signals often requires transmission schemes that lose unambiguous Doppler velocity and range resolution to achieve orthogonality [3].

Waveform coding is commonly used in radars to achieve unique waveform recognition [4]. In addition, such coding can be used to achieve joint sensing and communication systems [5], [6]. Particularly, phase modulated continuous waveforms (PMCW) have been used to achieve mutual orthogonality between waveforms in the MIMO systems and enhance the robustness of the radar against interference [7]. However, any PMCW waveform suffers from poor Doppler tolerance, and its usage requires a high sampling frequency in the receiver. To overcome the limitations of both LFMCW and PMCW, applying phase-coding to LFMCW has become a notable alternative.

Phase-coded frequency modulated continuous waveforms (PC-FMCW), where coding is done over the time duration of the chirp (code controls the phase changes inside the sweep), have been investigated to enhance the mutual orthogonality of the waveform and achieve simultaneous transmission for the MIMO systems while keeping the advantages of LFMCW [8]–[10]. For the PMCW applications, different phase code families are optimized for providing good sensing performance (low sidelobes, certain Doppler tolerance) [11]. However, these properties do not hold after using a chirp as a carrier for these codes and finding the suitable code families to use with PC-FMCW becomes important.

The objective of this paper is to investigate how different code families affect the sensing performance of PC-FMCW waveform. To achieve this task, we rewrite the signal model and pre-processing of PC-FMCW signal in Section II. Then in Section III, we examine the ambiguity function of PC-FMCW and the shearing effect of LFM on its ambiguity function. The comparison of the range profiles corresponding to PC-FMCW modulated with different code families and their corresponding integrated sidelobe level (ISL) are given in Section IV. Finally, the concluding remarks are highlighted in Section V.

II. Signal Model

Linear frequency modulated continues waveform can be written as:

$$x_{\text{fmcw}}(t) = \exp\left(j\left(2\pi f_c t + \pi\gamma t^2\right)\right), \quad t \in [0, T], \tag{1}$$

where f_c is the carrier frequency of the radar, B and T are the bandwidth and the time duration of the chirp respectively, and $\gamma = B/T$ denotes the chirp rate. Assume a phase-coded signal $s(t)$ is used to modulate the LFMCW signal (1). Then the transmitted waveform for PC-FMCW can be written as:

$$x_{\text{t}}(t) = s(t)\exp\left(j\left(2\pi f_c t + \pi\gamma t^2\right)\right). \tag{2}$$

In this study, we consider binary phase shift keying (BPSK) as a phase modulation scheme where the phase changes between $\{0, \pi\}$ according to the phase sequence ϕ_n. Then the phase-coded signal can be represented as:

$$s(t) = \sum_{n=1}^{N_c} e^{j\phi_n}\,\text{rect}\left(\frac{t-(n-1/2)T_c}{T_c}\right), \tag{3}$$

where $\text{rect}(t)$ is the rectangle function, N_c is the number of chips within one chirp, $T_c = T/N_c$ is the chip duration. Then the bandwidth of the code signal can be calculated as $B_c = N_c/T$. When the transmitted signal (2) is reflected from a target at a range R_0 moving with a constant radial velocity v_0, the round trip delay between radar and target can be given as:

$$\tau_0(t) = \frac{2\left(R_0 + v_0 t\right)}{c}, \tag{4}$$

where c is the speed of light. For the narrow band, the received signal is a linearly delayed copy of the transmitted signal with a corresponding Doppler shift. Accounting propagation and back-scattering effects by complex coefficient η, the received signal can be represented as:

$$x_{\mathrm{r}}(t) = \eta\, x_{\mathrm{t}}(t - \tau_0(t)) + n(t) \tag{5}$$

where $n(t)$ represents the received noise signal. The received signal acquisition time T_{aq}= $[0, T{+}T_r]$, where T_r is the pulse repetition interval and for the continuous wave T_r=T. In the white noise scenario, the optimum receiver that jointly maximizes signal-to-noise ratio (SNR) for each range-Doppler hypothesis is the matched filter [12]. After down-conversion with the carrier tone to the base-band, the matched filter receiver convolves the received signal with the complex conjugate of the transmitted signal as:

$$x_{\mathrm{MF}}(t) = \int_{-\infty}^{\infty} x_{\mathrm{r}}(k)\, x_{\mathrm{t}}{}^{*}(t-k)\, dk, \tag{6}$$

where $(\cdot)^*$ denotes the complex conjugate. The matched filter output contains the range information about the target.

Note that conventional matched filtering requires the sampling of the signal with its full band. As a result of high sampling demands, conventional matched filtering is not suitable for radars where the processing power is limited. To overcome this problem, the matched filter can be realized via filter bank after dechirping, or it can be approximated by using the group delay filter receiver. Both of these receiver approaches significantly decrease the sampling requirements of analog-to-digital converter (ADC) [13]. In this study, we focus on the matched filter and the ambiguity function to set the boundaries for the sensing performance of the waveform with different code families.

III. Ambiguity Functions

In this section, we use the ambiguity function, which is a principal tool for studying radar waveforms and corresponds to the outcome of the matched filter. The ambiguity function of signal $x(t)$ can be calculated as a linear (aperiodic) convolution of a signal with its time-delayed and frequency-shifted replica:

$$|\,\chi(x(t);\tau,f_d)\,| = \left| \int_{-\infty}^{\infty} x(t)\, x^{*}(t-\tau) e^{j2\pi f_d t}\, dt \right|, \tag{7}$$

where f_d represents the Doppler frequency. The ambiguity function determines the range-Doppler resolution of the transmitted signal for selected system parameters. In this particular example, we select $B = 10$ MHz and $T = 25.6$ μs for the LFM signal. Moreover, we use $N_c = 16$ chips within one chirp duration so that the chirp bandwidth becomes $B_c = 0.62$ MHz for the phase-coded signal, and no repetitions of the code over a duration of the signal are performed. As mentioned in the introduction, one of the advantages of LFMCW signal is its high range resolution and good Doppler tolerance. This behaviour can be seen in Fig. 1 a, where the ambiguity function of LFM signal is demonstrated. However, the ambiguity function of PMCW has poor Doppler tolerance

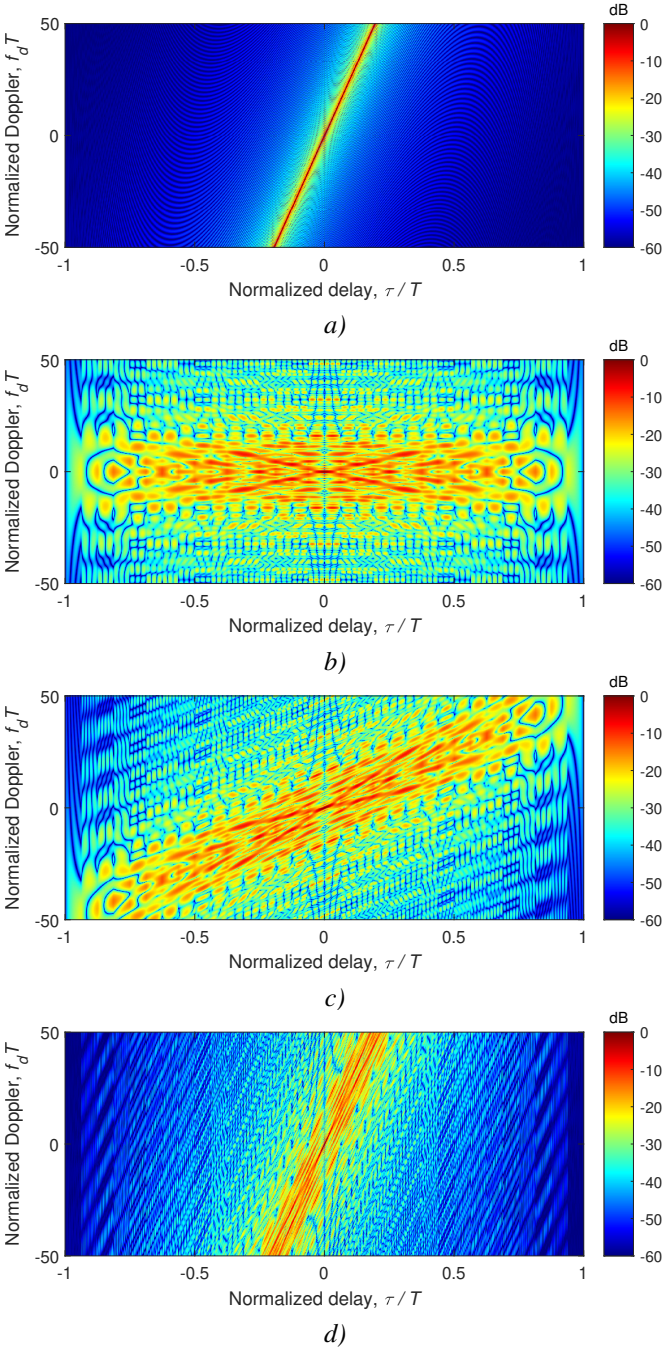

Fig. 1. Ambiguity functions of a) LFM B=10 MHz b) PMCW c) PC-FMCW B=2 MHz d) PC-FMCW B=10 MHz. The shearing effect of LFM on the ambiguity function of phase-coded signal with $B_c = 0.62$ MHz is observed

as shown in Fig. 1 b. As a result, the PMCW signal is very sensitive to Doppler frequency shifts caused by the target motion, and it often requires a special process for moving targets to compensate for the poor Doppler tolerance.

In [12], it is proved that adding the linear frequency modulation, which is equivalent to a quadratic-phase modulation, shears the resulting ambiguity function. This main property of the ambiguity function can be represented as:

$$\left|\,\chi(s(t)\exp\left(j\pi\gamma t^2\right);\tau,f_d)\,\right| \Longleftrightarrow |\,\chi(s(t);\tau,f_d-\gamma\tau)\,|\,. \tag{8}$$

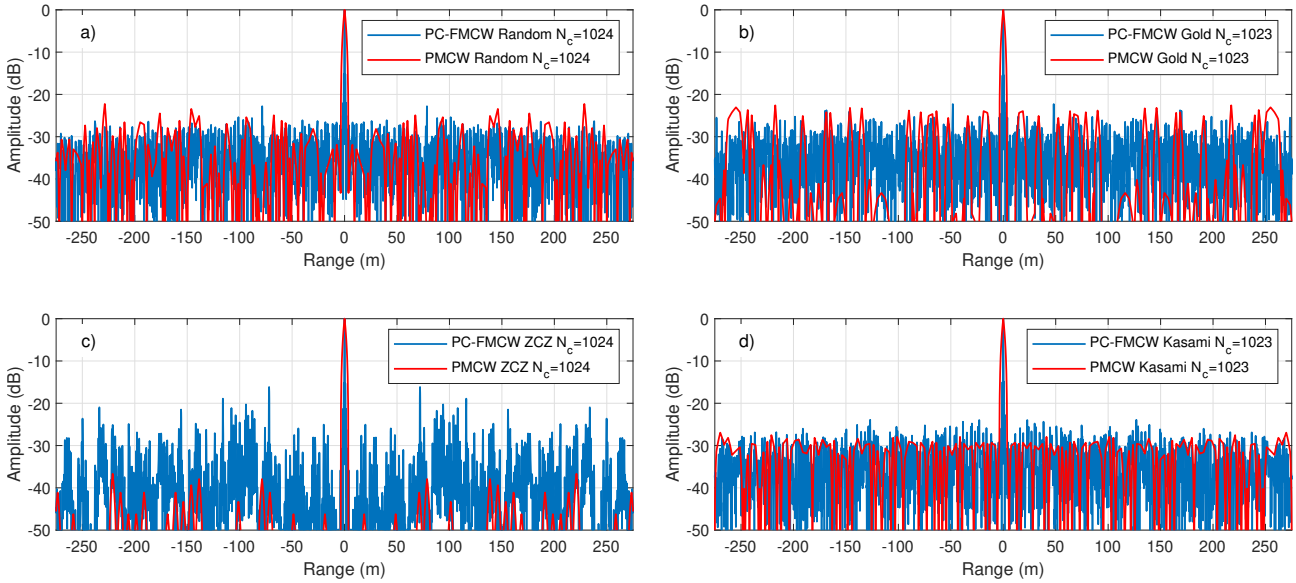

Fig. 2. Range profile comparison of PMCW and PC-FMCW with different code families; a) Random b) Gold c) ZCZ d) Kasami

Consequently, the ambiguity function of PC-FMCW is a sheared version of the coding signal ambiguity function and this shearing effect is proportional to the chirp slope. We observe this phenomenon in Fig. 1 c, where the ambiguity function of PC-FMCW with $B = 2$ MHz is demonstrated. Due to this shearing effect, the ambiguity function of PC-FMCW has a range-Doppler coupling similar to LFMCW. As shown in Fig. 1 d, the Doppler tolerance of PC-FMCW has substantially improved compared to PMCW by increasing the chirp bandwidth to $B = 10$ MHz. Note that the parameters selected herein are different from typical automotive radars ($B = 300$ MHz) to observe the shearing effect clearly. By increasing the chirp bandwidth to typical values, PC-FMCW keeps the advantages of LFMCW such as high range resolution, Doppler tolerance and constant PAPR while having the advantage of waveform coding and mutual orthogonality.

IV. Range Profile Comparison

In this section, we compare the zero Doppler cut (range profile) of the ambiguity functions of PC-FMCW modulated with different code families, namely random, Gold, zero correlation zone (ZCZ) and Kasami codes [11], which have different sidelobe levels. Although these codes are optimized for periodic auto-correlation properties, they still exhibit reasonable aperiodic auto-correlation properties. We consider an automotive radar scenario where the transmitting PC-FMCW has a chirp duration $T = 25.6$ μs with a carrier frequency $f_c = 77$ GHz, and chirp bandwidth $B = 300$ MHz. The BPSK sequence is used as a phase-coded signal to modulate LFMCW. Hence, the amplitude of the phase-coded signal is constant and changes between $\{-1, 1\}$. We use $N_c = 1024$ number of chips per chirp. Thus the bandwidth of the code signal becomes $B_c = N_c/T = 40$ MHz.

The ambiguity functions of PC-FMCW and PMCW are simulated by using the same code families. The comparison of the range profiles with the zero Doppler cut is demonstrated in Fig. 2. It can be seen that the random code provides ~ 23 dB dynamic range with the chosen system parameters while the Gold code provides the same dynamic range with lower sidelobes in the far range. Moreover, it is observed that the range profile of the code itself (PMCW) is changed essentially after modulating with the chirp signal (PC-FMCW). This behaviour can be seen especially for the ZCZ code in Fig. 2 c. The ZCZ code, as the name implies, is a code that tries to find a zone with zero correlation, and the range profile of the ZCZ code has sidelobes less than ~ -40 dB close to the main lobe. However, adding linear frequency modulation alters the code property, and its sidelobe is raised to ~ -15 dB. Thus, the design of optimal code for PC-FMCW is a problem to be considered in future. As for the Kasami code, we see that it has a dynamic range of ~ 30 dB without chirp and modulating with chirp increases its dynamic range to ~ 23 dB with a slightly different range profile than the Gold code.

Next, we assess the sidelobe levels of different code families by using integrated sidelobe level (ISL). Since we consider automotive radar application, we only take into account ISL between range interval ± 250 meter noted as the

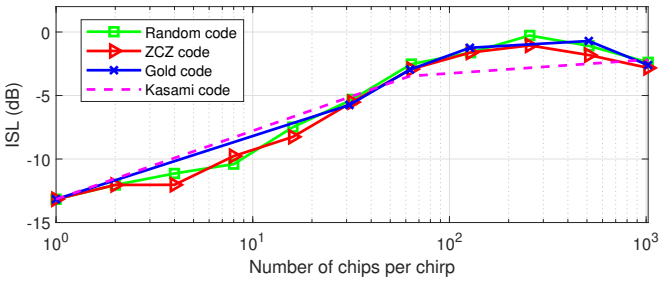

Fig. 3. Integrated side lobe level comparison of PC-FMCW with different code families

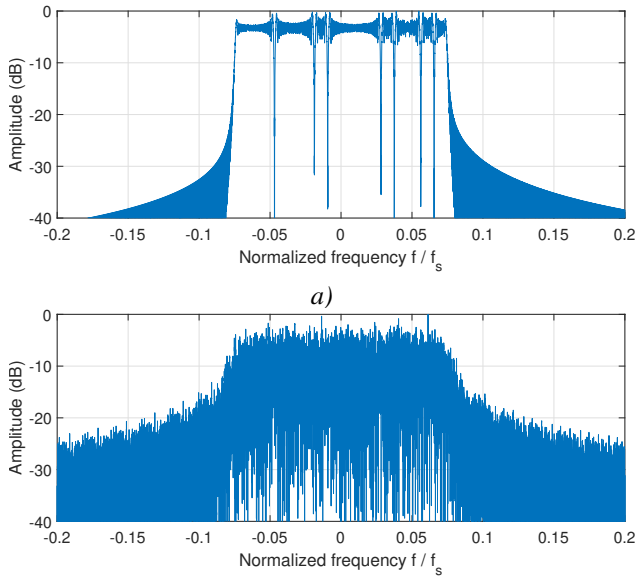

Fig. 4. Spectrum of the transmitted PC-FMCW with random phase-coded signal a) $N_c = 16$, relative code bandwidth $B_c/B = 0.002$ b) $N_c = 1024$, relative code bandwidth $B_c/B = 0.133$

interval $[r_1, r_4]$. Then ISL can be defined as [14]:

$$\mathrm{ISL} = 10\log_{10}\left(\frac{\int_{r_1}^{r_2} |\chi(\tau,0)|^2\,\mathrm{d}\tau + \int_{r_3}^{r_4} |\chi(\tau,0)|^2\,\mathrm{d}\tau}{\int_{r_2}^{r_3} |\chi(\tau,0)|^2\,\mathrm{d}\tau}\right), \tag{9}$$

where the interval $[r_2, r_3]$ defines the main lobe, and $\chi(\tau, 0)$ is the zero Doppler cut of the ambiguity function of signal $x(t)$.

ISL of PC-FMCW with investigated code families are compared and illustrated as a function of the number of chips per chirp in Fig. 3. It is seen that ISL of investigated code families are comparable, and their ISL raises as the number of chips per chirp increases. This behaviour is expected because the bandwidth of the code becomes comparable to chirp bandwidth and spectrum leakage outside of the chirp bandwidth leads to increased sidelobes. To illustrate this issue, we compare the relative bandwidth of the code with chirp bandwidth as B_c/B in Fig. 4. It can be observed that the power of leakage outside of the chirp bandwidth increased ~ 20 dB as the relative code bandwidth changed from 0.002 to 0.133. Thus, the relative code bandwidth limits the sensing performance and should be considered in the system design.

V. Conclusion

The ambiguity function of PC-FMCW is investigated. Modulating with the chirp signal shears the ambiguity function of phase-coded signal, and thus PC-FMCW has Doppler tolerance and high range resolution similar to LFMCW. The zero Doppler cuts of the ambiguity function are shown for random, Gold, ZCZ and Kasami code, and their sensing performance has been compared. It has been demonstrated that the sidelobe values in the range profile of PC-FMCW might be essentially different from the sidelobe levels of code auto-correlation function; different codes with different auto-correlation functions provide very similar sensing performance for PC-FMCW. The demonstrated performance can be used as a boundary for any practical realization of the receiver design. The utilization of codes mutual orthogonality for self-interference suppression in the MIMO systems will be presented elsewhere.

Acknowledgment

Part of this research activity was performed within the TU Delft Industry Partnership Program (TIPP), which is funded by NXP Semiconductors N.V. and Holland High Tech Systems and Materials (TKIHTSM/18.0136) under the project 'Coded Radar for Interference Suppression in Super-Dense Environments' (CRUISE).

References

[1] S. D. Blunt and E. L. Mokole, "Overview of radar waveform diversity," *IEEE Aerospace and Electronic Systems Magazine*, vol. 31, no. 11, pp. 2–42, 2016.

[2] U. Kumbul, F. Uysal, C. S. Vaucher, and A. Yarovoy, "Automotive radar interference study for different radar waveform types," *IET Radar, Sonar & Navigation*, vol. 16, no. 3, pp. 564–577, 2022. [Online]. Available: https://ietresearch.onlinelibrary.wiley.com/doi/abs/10.1049/rsn2.12203

[3] S. Sun, A. P. Petropulu, and H. V. Poor, "Mimo radar for advanced driver-assistance systems and autonomous driving: Advantages and challenges," *IEEE Signal Processing Magazine*, vol. 37, no. 4, pp. 98–117, 2020.

[4] S. Alland, W. Stark, M. Ali, and M. Hegde, "Interference in automotive radar systems: Characteristics, mitigation techniques, and current and future research," *IEEE Signal Processing Magazine*, vol. 36, no. 5, pp. 45–59, 2019.

[5] F. Liu, C. Masouros, A. Petropulu, H. Griffiths, and L. Hanzo, "Joint radar and communication design: Applications, state-of-the-art, and the road ahead," *IEEE Transactions on Communications*, vol. 68, pp. 3834–3862, 2020.

[6] L. G. de Oliveira, B. Nuss, M. B. Alabd, A. Diewald, M. Pauli, and T. Zwick, "Joint radar-communication systems: Modulation schemes and system design," *IEEE Transactions on Microwave Theory and Techniques*, vol. 70, no. 3, pp. 1521–1551, 2022.

[7] A. Bourdoux and M. Bauduin, "Pmcw waveform cross-correlation characterization and interference mitigation," in *2020 17th European Radar Conference (EuRAD)*, 2021, pp. 164–167.

[8] R. Feger, H. Haderer, and A. Stelzer, "Optimization of codes and weighting functions for binary phase-coded fmcw mimo radars," in *2016 IEEE MTT-S International Conference on Microwaves for Intelligent Mobility (ICMIM)*, 2016, pp. 1–4.

[9] F. Uysal, "Phase-coded fmcw automotive radar: System design and interference mitigation," *IEEE Transactions on Vehicular Technology*, vol. 69, no. 1, pp. 270–281, 2020.

[10] U. Kumbul, N. Petrov, C. S. Vaucher, and A. Yarovoy, "Smoothed phase-coded fmcw: Waveform properties and transceiver architecture," 2022. [Online]. Available: https://arxiv.org/abs/2203.07508

[11] E. García, J. A. Paredes, F. J. Álvarez, M. C. Pérez, and J. J. García, "Spreading sequences in active sensing: A review," *Signal Processing*, vol. 106, pp. 88 – 105, 2015.

[12] N. Levanon and E. Mozeson, *Radar signals*. NJ, USA: John Wiley & Sons, Ltd, 2004.

[13] U. Kumbul, N. Petrov, C. S. Vaucher, and A. Yarovoy, "Receiver structures for phase modulated fmcw radars," in *2022 16th European Conference on Antennas and Propagation (EuCAP)*, 2022, pp. 1–5.

[14] M.-E. Chatzitheodoridi, A. Taylor, and O. Rabaste, "A mismatched filter for integrated sidelobe level minimization over a continuous doppler shift interval," in *2020 IEEE Radar Conference (RadarConf20)*, 2020, pp. 1–6.